Carbohydrate Polymers 98 (2013) 514–521

Contents lists available at SciVerse ScienceDirect

Carbohydrate Polymers

journal homepage: www.elsevier.com/locate/carbpol

TG-MS analysis for thermal decomposition of cellulose under different atmospheres

Dekui Shen[a], Jiangming Ye[b], Rui Xiao[a,*], Huiyan Zhang[a]

[a] Key Laboratory of Energy Thermal Conversion and Control, Ministry of Education, School of Energy and Environment, Southeast University, Nanjing 210096, China
[b] Nanjing Institute of Technology, Nanjing 211167, China

ARTICLE INFO

Article history:
Received 26 March 2013
Received in revised form 23 May 2013
Accepted 18 June 2013
Available online 26 June 2013

Keywords:
Cellulose
TG-MS
Pyrolysis
Oxidation
Kinetic model

ABSTRACT

Cellulose degradation under inert (He) and oxidative atmospheres (7% O_2, 20% O_2 and 60% O_2) was investigated through thermogravimetric (TG) equipped with mass spectroscopy (MS) system. Two mass loss stages were observed for cellulose degraded under oxidative atmosphere, where the first mass loss stage is close to that under inert atmosphere, and the second one designated to char oxidation was enhanced by the increased oxygen concentration. The evolution of prominent volatiles including furfural, acetone, 2/5-hydromethyl furfural, formaldehyde, CO and CO_2 was examined considering the influence of oxygen concentration. The plateau for mass loss and evolution of some volatiles leads to the difficulty to determine the division-point for the two stages. However, the fitting parameter (Dev%) around 5% confirms the applicability of the proposed two-stage kinetic model accounting for partial pressure of oxygen.

1. Introduction

Sustainable development of human society is highly demanding the exploitation of clean and renewable energy sources, due to the huge need of fossil fuels and the higher sensibility toward environment protection from conventional energetic system. Biomass, a term for all organic materials from plants, is being situated at the center of scientific and industrial interest with regard to its characteristics as renewable, widely distributed, indigenous, CO_2-neutral and so on (Blasi, 2008; McKendry, 2002a,b). In addition, it is the only renewable source for liquid fuels and chemicals (Mettler, Vlachos, & Dauenhauer, 2012; Sanderson, 2006). Pyrolysis is established as a promising method for converting biomass to liquid fuel and chemical feedstock, which is also involved in other thermo-chemical technologies (e.g., gasification, combustion, and carbonization) as the initial step. More and more global attentions were attracted on the fundamentals of pyrolysis chemistry of biomass and its application (McKendry, 2002a,b; Mettler et al., 2012).

The chemistry of individual components (e.g., cellulose, hemicellulose and lignin) has been generally focused for over the past five decades for better understanding of biomass pyrolysis (Mettler et al., 2012). Cellulose, uniformly consisting of glucopyranose linearly polymerized through Beta-1, 4-glycosidic bond with the specific polymerization degree varied with origins, is the most abundant constituent (over 50 wt%) in biomass over the other components (Dumitriu, 2005; McKendry, 2002a,b). A large number of research works on pyrolysis of cellulose were reported in the literature and extensively overviewed by several researchers (Antal & Varhegyi, 1995; Blasi, 2008; Lin, Cho, Tompsett, Westmoreland, & Huber, 2009; Mettler et al., 2012), regarding the kinetic chemistry, transport mechanism, product distribution influenced by reactors, experimental conditions and catalytic effects. Most of the reported studies were concentrated on the pyrolytic behavior of cellulose under inert atmosphere, but rarely under other atmospheres (e.g., oxygen, CO_2 and H_2O).

Recently, the degradation of biomass and cellulose under oxygen-containing molecules attracted the growing attention of global researchers, in order to gain better understanding of the fundamentals of CO_2, oxidative and steam gasification, combustion and oxy/fuel combustion and help optimize operating conditions for the process. Information of mass loss of biomass under oxidative atmospheres was intensively discussed, together with the erection of apparent kinetic models for simulating the process (Amutio, Lopez, Aguado, Artetxe, Bilbao, & Olazar, 2012a; Branca & Blasi, 2004; Shen, Gu, Luo, Bridgwater, & Fang, 2009). The heat and mass transport phenomena and surface chemi-sorption were ignored for the first mass loss stage (pyrolysis process) during oxidative pyrolysis of biomass, while those for second stage (char oxidation) were estimated and well-incorporated into the intrinsic kinetic models (Gómez-Barea, Ollero, & Arjona, 2005; Li & Brown, 2001; Ollero,

* Corresponding author. Tel.: +86 25 83795726; fax: +86 25 83792828.
E-mail addresses: ruixiao@seu.edu.cn, 101011398@seu.edu.cn (R. Xiao).

0144-8617/$ – see front matter.
http://dx.doi.org/10.1016/j.carbpol.2013.06.031

Serrera, Arjona, & Alcantarilla, 2002). It needs to be noted that the chemical information concerning the volatile evolution during the whole process was insufficiently investigated, which might help improve the existed kinetic models. Moreover, the study on cellulose oxidative degradation is scarcely reported in comparison to that of biomass (Tihay, Boulnois, & Gillard, 2011).

A set of experiments on cellulose degradation under inert and oxidative atmospheres were carried out in order to fill the knowledge gap. Mass loss information together with the evolution of prominent volatiles was examined through TG-MS system (Thermogravimetric Analyzer-Mass Spectroscopy). A kinetic model considering the partial pressure of oxygen was proposed to simulate the process.

2. Materials and methods

2.1. Materials

Cellulose powder was bought from Sigma Aldrich. The content of C, H and O (dry basis) was 41.20%, 6.54% and 52.26%, while proximate analysis showed the content of volatile, fixed carbon and ash (dry basis) as 90.9%, 2.48% and 0.18%. The sample was milled and sieved to obtain particles less than 50 μm in diameter, in order to prevent the temperature gradient in sample bed during pyrolysis. The sample was dried in an oven at 105 °C for 5 h prior to the experimental runs.

2.2. Experimental setup

2.2.1. Equipment

The experimental system, consisting of Thermogravimetric Analyzer (Netzsch STA 409) coupled with Mass Spectroscopy (PFEIFFER VACUUM QMS422). Adjustment of the heating rate of TGA is up to 50 K/min, while the temperature limit was about 1500 °C. The atmosphere in the TG furnace could be changed according to the requirement. The electron ionization voltage for MS could be operated from 0 to 220 eV and the identified ions (m/z) were in the range of 0–500 a.m.u. The TG analyzer was connected to a mass spectrometer (MS) through a tube, and all interfaces were wrapped with heating wire to prevent condensation of the evolved volatiles.

2.2.2. Procedure

About 10 mg of sample was loaded into an aluminum crucible and placed on the sample holder in the TG furnace. The sealed furnace was evacuated three times in order to remove all air. In order to identify prominent ions with m/z in the range of 0–200, a preliminary broad scan was performed for the sample in TGA at a heating rate of 20 K/min, while the electron ionization voltage of the MS was set at 70 eV and temperature of the heating wire was maintained at 200 °C. It was estimated that the lower heating rate could facilitate the evolution of low-molecular-weight compounds and ions identified in the preliminary scan helped to obtain better resolution for MS scanning during the pyrolysis experiments (Widyawati, Church, Florin, & Harris, 2011). The signals from the mass spectra of 18, 28, 30, 44, 60, 74, 96 and 126 (m/z) were identified as the major contributors from the specific evolved gases and volatiles (H_2O, CO, CH_2O, CO_2, acetic acid/hydroxyl acetaldehyde, pyruvicaldehyde, furfural, and 2/5-hydroxymethyl furfural), according to the database of National Institute of Standards and Technology (Sanchez-Silva, Lopez-Gonzalez, Villasenor, Sanchez, & Valverde, 2012) and relevant previous study (Lv & Wu, 2012).

Prior to experimental runs, mass spectroscopy was firstly set to monitor the variation of signals of the selected prominent ions (m/z) from the preliminary scan. Once the reaction atmosphere in TG furnace was sustained, the sample started to be heated from room temperature to the target temperature at a fixed heating rate. The mass spectra intensities were normalized by the initial sample mass and the baseline was also subtracted from the measurements for each experiment. TG data could be correlated with the mass spectra considering the 1-min lag due to the migration of evolved gases from the TG to the MS. Experimental conditions are set as: oxygen concentration: 0%, 7%, 20% and 60%, temperature: from 20 to 800 °C, heating rate: 20 K/min and total flow rate of reaction gas: 100 ml/min regardless of oxygen concentration. Three times for each experiment were carried out.

3. Results and discussion

3.1. TG and DTG analysis

The mass loss history of cellulose at heating rate of 20 K/min under different atmospheres was tracked as shown in Fig. 1(a). Only one sharp mass loss stage between 280 °C and 380 °C (over 90% mass loss of original material in Table 1) was found for cellulose degraded under inter atmosphere (He). Under oxidative atmosphere, another mass loss stage located in the high temperature region (from 440 °C to 580 °C) could be observed, which was enhanced by the oxygen concentration (Fig. 1(b)). The two mass loss stages for the degradation of biomass and its constituents under oxidative atmosphere is commonly designated to pyrolysis process of original materials in low temperature region and oxidation of char formed by primary pyrolysis reaction(s) (Amutio et al., 2012a;

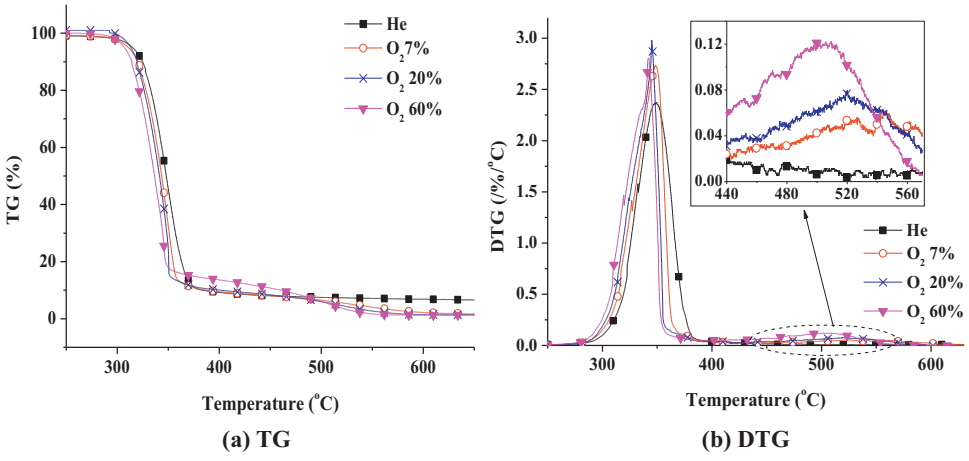

Fig. 1. TG and DTG curves of cellulose degradation under different atmospheres.

Table 1
Characteristics of mass loss process of lignin decomposed at different atmospheres.

Atmosphere	T^0 (°C)	T^1 (°C)	dX/dt^1 (%/°C)	X^1 (%)	T^b (°C)	dX/dt^b (%/°C)	X^b (%)	T^2 (°C)	dX/dt^2 (%/°C)	X^2 (%)	T^f (°C)	X^f (%)
0% O_2 (He)	262	350	2.37	45.62	–	–	–	–	–	–	469	7.78
7% O_2	269	348	2.73	39.18	443	0.0199	8.31	537	0.055	5.21	611	1.84
20% O_2	271	345	2.98	40.70	419	0.0271	9.37	520	0.079	4.64	592	1.42
60% O_2	267	342	2.89	39.15	389	0.0514	14.1	509	0.134	4.99	567	1.38

0, the point of the commencement of lignin degradation after the drying stage when dX/dt > 0.01%/°C.
1, the point at the first peak of mass loss rate.
b, the bottom of mass loss rate between the two peaks.
2, the point at the second peak of mass loss rate.
f, the point of the completion of lignin degradation when dX/dt < 0.01%/°C.

Bilbao, Mastral, Aldea, & Ceamanos, 1997; Branca & Blasi, 2004; Liu, 2002; Shen et al., 2009; Vaĭrhegyi, Sebestyeĭn, Czegeĭny, Lezsovits, & Könczöl, 2012).

Intensity of the first mass loss peak is notably strengthened with the presence of oxygen (2.37%/°C in Table 1), while the value is slightly affected by the oxygen content (around 2.8%/°C for different oxygen concentrations). The temperature corresponding to the first mass loss peak (peak temperature) is not varied regardless of surrounding atmosphere. The second mass loss stage assigned to char oxidation is significantly enhanced with the oxygen concentration (Fig. 1(b)), since the peak value of mass loss rate was increased and the peak temperature shifted to low temperatures (Table 1).

A remarkable plateau between the two mass loss stages (approximately from 380 °C to 440 °C) could be found (Fig. 1(a)), which is attributed to the co-existence of pyrolysis and char oxidation (Liu, 2002). The bottom of DTG curves located in the mass loss plateau under oxidative atmosphere could apparently imply the transition point of pyrolysis-dominant process to char oxidation dominant one. The first mass loss stage (pyrolysis process) is found to be shortened with the increased oxygen concentration (269–443 °C for 7% O_2, 271–419 °C for 20% O_2 and 267–389 °C for 60% O_2 in Table 1). It needs to be noted that the solid residue corresponding to the bottom of DTG curve was increased with the oxygen concentration (Table 1). One of the possible explanations is that the presence of oxygen promotes the condensation reaction during the pyrolysis process (the first mass loss stage). As a result, more char residue was produced for mass loss contribution of the second stage. Another explanation is that char oxidation (the second mass loss stage) was significantly enhanced by oxygen concentration, leading to the dominance of char oxidation in the mass loss plateau shifting to lower temperatures. The mass loss plateau of cellulose degradation under oxidative atmosphere would attract more and more attentions due to the ambiguity of co-existence of the chemical reactions.

3.2. Evolution of prominent volatiles and light gases

The evolved volatile passed through mass spectroscopy (MS) might be broken into a few of fragments, leading to the difficulty for designating the ion to specific compound. The library attached to the MS system favors the identification of compound from the ion(s), which is widely employed in previous studies (Huang, Kuan, Chieuh, & Lo, 2011; Lv & Wu, 2012; Sanchez-Silva et al., 2012; Shen et al., 2012; Widyawati et al., 2011). The intensity of selected ions (18, 28, 30, 44, 60, 74, 96 and 126 m/z), designated to water, CO, formaldehyde, CO_2, acetic acid/hydroxyl acetaldehyde, 1-hydroxy-2-propanone, furfural and 2/5-hydromethyl-furfural, was tracked by MS for cellulose degradation under both inert and oxidative atmospheres.

3.2.1. Prominent volatiles

The evolution of volatiles corresponding to the ions of 60, 74, 96 and 126 m/z was shown in Fig. 2, while some characteristic points were summarized in Table 2. The ion of 60 m/z might be originated from both acetic acid and hydroxyl acetaldehyde (Lv & Wu, 2012;

Table 2
Characteristics for the evolution of prominent volatiles and light gases from cellulose degradation under inert and oxidative atmospheres identified by MS analysis.

Atmosphere		H_2O	CO	CO_2	FA	GAA	PA	FF	5-HFM
He	Main evolution range (°C)	270–493	260–460	266–473	269–497	272–496	272–492	268–495	261–481
	T^1 (°C)	342	350	351	340	348	349	340	346
	Int.^{1} ($\times 10^{12}$ a.u./mg)	567	76	94.2	47.1	3.21	0.95	25.7	1.23
7% O_2	Main evolution range (°C)	265–470	280–626	263–624	261–473	269–472	–	262–477	–
	T^1 (°C)	335	334	335	330	338	–	330	–
	Int.^{1} ($\times 10^{12}$ a.u./mg)	916	188	1980	29.7	0.79	–	12.7	–
	T^2 (°C)	–	544	542	–	–	–	–	–
	Int.^{2} ($\times 10^{12}$ a.u./mg)	–	70.3	81.4	–	–	–	–	–
20% O_2	Main evolution range (°C)	252–488	270–612	264–608	261–477	271–469	–	263–467	–
	T^1 (°C)	326	324	326	320	327	–	324	–
	Int.^{1} ($\times 10^{12}$ a.u./mg)	2010	432	4539	55.7	1.04	–	15.6	–
	T^2 (°C)	–	530	528	–	–	–	–	–
	Int.^{2} ($\times 10^{12}$ a.u./mg)	–	117	204	–	–	–	–	–
60% O_2	Main evolution range (°C)	259–498	267–579	255–576	264–472	265–452	–	261–462	–
	T^1 (°C)	322	321	322	319	325	–	322	–
	Int.^{1} ($\times 10^{12}$ a.u./mg)	1920	383	3550	67.7	0.94	–	18.0	–
	T^2 (°C)	–	515	511	–	–	–	–	–
	Int.^{2} ($\times 10^{12}$ a.u./mg)	–	126	382	–	–	–	–	–

0, evolution range is the temperature interval between when evolution intensity is firstly larger than 1% of the peak value and finally smaller than 1% of the peak value.
Int. is the abbreviation of intensity.
1, the point at the first peak of gas evolution.
2, the point at the second peak of gas evolution.
–, the intensity of the spectra is no more than 1×10^{-13} during the scanning period.

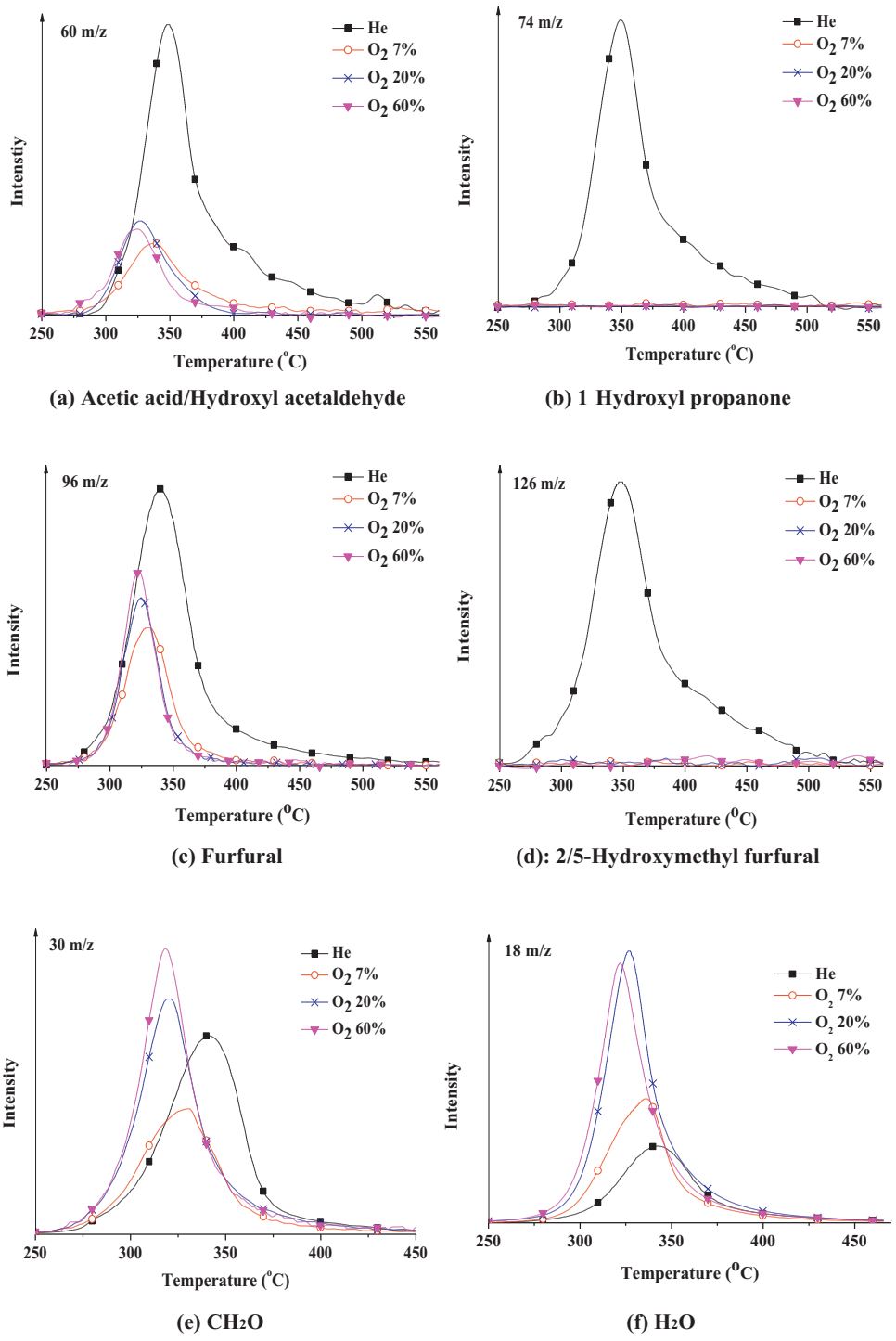

Fig. 2. Evolution of prominent volatiles from cellulose degradation under different atmospheres.

Shen & Gu, 2009). Hydroxyl acetaldehyde (HAA) is considered to be the remarkable product from cellulose pyrolysis. Therefore, the contribution of HAA is dominant over that acetic acid under inert atmosphere (Fig. 2(a)). Under oxidative atmosphere, only one peak was observed in the low temperature stage, intensity of which was significantly decreased compared to that under inert atmosphere due to the oxidation of HAA in gas phase. However, the peak intensity was firstly increased with the oxygen concentration and then decreased (0.79×10^{-12} a.u./mg for 7% O_2, 1.04×10^{-12} a.u./mg for 20% O_2 and 0.94×10^{-12} a.u./mg for 60% O_2), since the oxygen promoted the formation of acetic acid from original material, which might be further oxidized to be CO or CO_2 with more addition of oxygen.

The evolution of furfural assigned to the ion 96 m/z under different atmospheres was similar to that of ion 60 m/z, where only one peak was observed in the low temperatures stage (Fig. 2(c)). Also, the presence of oxygen prohibited the evolution of furfural with regard to the remarkable decline of peak intensity from 25.7×10^{-12} a.u./mg for He (0% O_2) to 12.7×10^{-12} a.u./mg for 7% O_2 (Table 2). However, a slight increase of peak intensity of furfural evolution could be found with the increased oxygen concentration. Two possible phenomena might be involved: (1) the

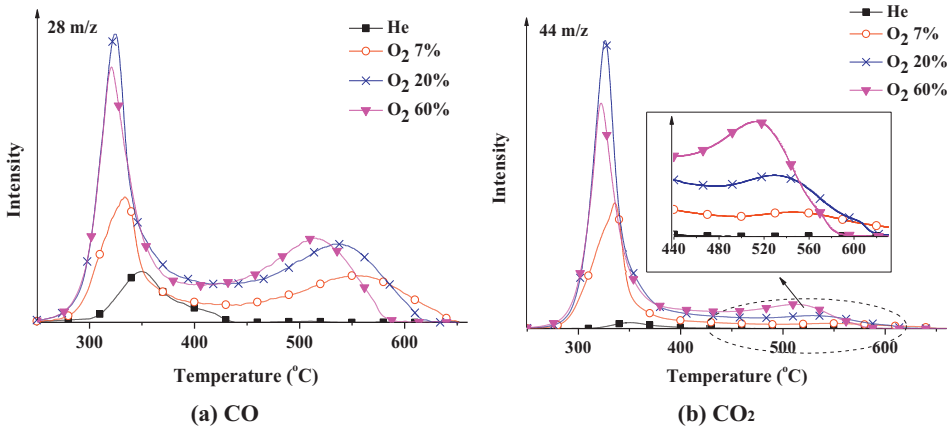

Fig. 3. Evolution of light gases from cellulose degradation under different atmospheres.

net evolution rate of furfural determined by (oxidative) pyrolysis of original materials and oxidation of furfural was increased with oxygen concentration; (2) furfural produced by oxidation of 2/5-hydroxymethyl-furfural (2/5-HMF) was enhanced by oxygen concentration. The latter explanation could be confirmed by evolution history of 2/5-HMF assigned to ion of 126 *m*/*z* (Fig. 2(d)). No notable evolution peak of 2/5-HMF could be observed under oxidative atmospheres, which might be consumed by oxidation reaction to produce furfural and light gases. Similarly, the ion of 74 *m*/*z* designated to 1-hydroxy-2-propanone was mostly oxidized as no significant signal was detected by MS under oxidative atmosphere (Fig. 2(b)).

It needs to be noted that the temperature at evolution peak of the four ions was in accordance with that on DTG curves under different atmospheres (Table 1 and Table 2), and none of them was detected in high temperature stage (char oxidation stage). The peak intensity of ion 96 *m*/*z* (furfural) in low temperature stage is much stronger than that of the other three ions (60, 74 and 126 *m*/*z*) under the same condition. In addition, the recorded evolution curve for furfural under oxidative atmosphere is remarkable over that of the other three ions, implying its outstanding ability of anti-oxidation.

Evolution of water assigned to ion of 18 *m*/*z* was shown in Fig. 2(e), where only one evolution stage was observed in low temperature stage under different atmospheres. The temperature at water evolution peak around 340 °C was close to that of DTG curves (350 °C), while a gap of about 100 °C between the temperature at water evolution peak and DTG curve was observed in the experiments of cellulose pyrolysis by Lin et al. (2009). The peak intensity was remarkably enhanced by the addition of oxygen (567×10^{-12} a.u./mg for He (0% O_2), 916×10^{-12} a.u./mg for 7% O_2, 2010×10^{-12} a.u./mg for 20% O_2 and 1920×10^{-12} a.u./mg for 60% O_2 in Table 2), due to the oxidation of volatiles in gas phase. The increment of oxygen exceeding the concentration of 20% has no significant effect on the evolution of water in low temperature stage. Evolution of water in high temperature stage under oxidative atmosphere was not notably detected, indicating the ignorable amount of hydrogen in char residue produced from low temperature stage (Amutio, Lopez, Aguado, Bilbao, & Olazar, 2012b). The analog evolution history of ion 30 *m*/*z* designated to formaldehyde was observed as shown in Fig. 2(f), where no significant evolution in high temperature stage was recorded. The evolution of formaldehyde in low temperature stage was enhanced by oxygen concentration, possibly due to the promotion of scission of C—C bond and oxidation of hydroxyl groups in original material.

3.2.2. *Light gases (CO and CO_2)*

The ions of 28 and 44 *m*/*z* assigned to CO and CO_2 were detected for cellulose degradation under different atmospheres (Fig. 3(a) and (b)), showing that the evolution stage(s) of both CO and CO_2 were consistent with the stage(s) of DTG curves (Fig. 1(b), Tables 1 and 2). The first evolution stage for both CO and CO_2 was enhanced with the addition of oxygen, due to the involvement of oxidation of evolved volatiles in gas phase (Table 2). The intensity of first evolution peak of CO was strengthened with the increased oxygen concentration (188×10^{-12} a.u./mg for 7% O_2 and 432×10^{-12} a.u./mg for 20% O_2), and the inflexion point of oxygen concentration for the effect might be located between 20% and 60% due to the decrease of peak intensity under 60% O_2 (383×10^{-12} a.u./mg). The similar phenomenon was also found for the first evolution stage of CO_2 (Fig. 3(b) and Table 2), indicating the complexity of chemical mechanism of the first stage involving both solid-phase and gas-phase reactions. For the second evolution stage, the enhancement with the increased oxygen concentration was observed for both CO and CO_2. This indicates that the char oxidation stage of cellulose degradation under oxidative atmosphere was accelerated by oxygen concentration mainly in forms of evolution of CO and CO_2 significantly determined by solid-phase reactions (Li & Brown, 2001; Moulijn & Kapteijn, 1995; Shen et al., 2012). It needs to be noted that the intensity of first evolution peak of both CO and CO_2 is stronger than that of second peak (Fig. 3(a) and (b)), because of the small amount of char residue (less than 10 wt% of original sample) derived from low temperature stage. The evolution intensity of CO_2 is prominent over that of other detected ions (Table 2), implying the dominance of CO_2 formation in both two stages of cellulose oxidative degradation. The evolution plateau of both CO and CO_2 between the first and second stage confirms the finding of co-existence of pyrolysis and char oxidation (Liu, 2002).

3.3. *Kinetic description for (oxidative) pyrolysis process*

The pyrolysis of biomass and its components under oxidative atmospheres in thermogravimetric (TG) system was observed to experience two prominent stages: solid pyrolysis in low temperature and char residue oxidation in high temperature. Some attempts were reported to successfully simulate the whole process (including the mass loss plateau) through the coupled consecutive reaction kinetic models (Amutio et al., 2012a; Branca & Blasi, 2004; Vaĭrhegyi et al., 2012), while the separate-stage kinetic models were proposed to describe the main mass loss stages during the process as this work did (Bilbao et al., 1997; Yoon, Pozivil, &

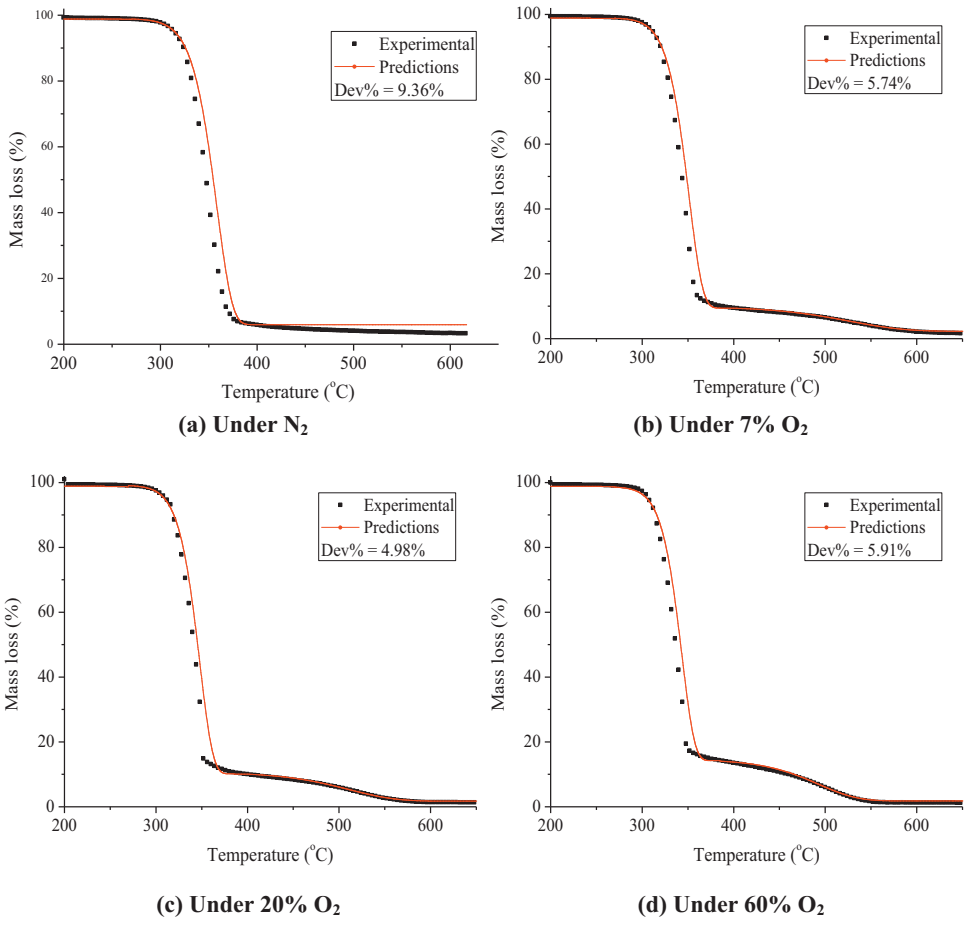

Fig. 4. Comparison on mass loss history of cellulose between experimental data and predictions under different atmospheres.

Steinfeld, 2012). The kinetics for the first stage of oxidative degradation of cellulose (pyrolysis process) was commonly expressed by first-order Arrhenius Law (Amutio et al., 2012a; Liu, 2002; Shen et al., 2009):

$$\frac{d\alpha_p}{dT} = A_p \quad \exp\left(-\frac{E_p}{RT}\right)(1-\alpha_p) \tag{1}$$

$$\alpha_p = \frac{m_0 - m_p}{m_0 - m_{p\infty}} \tag{2}$$

where α_p is the mass loss fraction for the first stage, m_0 is the initial mass of sample, $m_{p\infty}$ is the residue mass after the first stage.

For the second stage of oxidative degradation of cellulose (char oxidation), variation of partial pressure of oxygen was considered regarding its apparent influence on effective chemi-sorption of active sites of carbon matrix and therefore apparent chemical reactivity of char bed (Kashiwagi & Nambu, 1992; Li & Brown, 2001; Vaĭrhegyi et al., 2012). The expression for char oxidation rate can be illustrated as:

$$\frac{d\alpha_c}{dT} = A_c \exp\left(-\frac{E_c}{RT}\right)(1-\alpha_c)^{n_{\text{char}}}(P_{O_2})^{n_{\text{oxy}}} \tag{3}$$

$$\alpha_c = \frac{m_{c0} - m_c}{m_{c0} - m_{c\infty}} \tag{4}$$

where α_c is the mass loss fraction for the second stage, m_{c0} is the initial mass of char residue produced from the first stage which is equal to $m_{p\infty}$, and $m_{c\infty}$ is the residue mass after the second stage. The reaction order for char (n_{char}) during oxidation process was estimated to be around 1 for samples from willow, sewage sludge and wheat straw (Vaĭrhegyi et al., 2012). It is also stated by Chandrasekaran and Hopke that for the decomposition of polymers the reaction order could be assumed to be first order (Chandrasekaran & Hopke, 2012). As a result, the reaction order n_{char} in Eq. (3) was assumed to be 1. The method to determine the apparent parameters (A, E and n) for the kinetic model has been introduced in previous studies through logarithm transformation of the reaction rate equation and the correlated linear regression of experimental data (Fang, Shen, Li, Yu, Luo, & Cen, 2006; Liu, 2002; Ollero et al., 2003; Shen et al., 2012).

The deviation of predictions from the separate-stage reaction kinetic model is estimated as:

$$\text{Dev\%} = \frac{\sum_{i=1}^{i=N}\sqrt{(\alpha_{e,i}-\alpha_{m,i})^2/\alpha_{e,i}^2}}{N} \times 100\% \tag{5}$$

where α_e is the experimental mass loss fraction of solid and α_m is the predicted value. The comparison between experimental data and predicted results for the main mass loss stage(s) was shown in Fig. 4, and the deviation was mostly around 5% for different atmospheres.

The kinetic parameters for pyrolysis process of cellulose were comprehensively summarized by Lin et al. (Lin et al., 2009), where activation energy for the reaction was scattered in a large range (from 48 kJ/mol to 282 kJ/mol) due to the variation of sample origins, operating conditions or mathematical methods. The activation energy for pyrolysis of cellulose in this work was 207.8 kJ/mol, being close to those in previous works (Antal & Varhegyi, 1995; Lin et al., 2009; Tihay et al., 2011). It is worthy noting that the

Table 3
Parameters of the first-order separate-stage reaction kinetics for lignin gasification under different atmospheres.

Atmosphere	Temperature range (°C)	Mass loss range (%)	E (kJ/mol)	A (s^{-1})	n_{O_2}	R^2
First mass loss stage (pyrolysis process)						
0% O_2 (He)	270–420	98.87–8.86	207.8	2.99×10^{15}	–	0.973
7% O_2	270–400	99.10–9.53	216.9	2.97×10^{16}	–	0.9751
20% O_2	270–395	99.07–10.21	223.7	1.41×10^{17}	–	0.9596
60% O_2	270–390	98.62–14.09	228.1	4.70×10^{17}	–	0.9606
Second mass loss stage (char oxidation)						
7% O_2	400–610	9.53–2.04	88.7	8.44×10^{5}	2.26	0.9837
20% O_2	395–590	10.21–1.43	100.1	9.53×10^{5}	2.26	0.9854
60% O_2	390–565	14.09–1.39	115.1	1.10×10^{6}	2.26	0.9864

activation energy for pyrolysis process of cellulose under oxidative atmosphere was close to the value under inert atmosphere, and slightly increased with the oxygen concentration (216.9 kJ/mol for 7% O_2 and 228.1 kJ/mol for 60% O_2) (Table 3). A reverse trend of activation energy for pyrolysis process of cellulose against oxygen concentration was reported by Tihay et al. (2011), but the variation is not remarkable (200.5 kJ/mol for 5.25% O_2 and 181.1 kJ/mol for 21% O_2). It could be concluded that the presence of oxygen plays no significant role in pyrolysis process of cellulose in low temperature stage, although the stage was shortened with the increased oxygen concentration.

The kinetic description for cellulose-derived char oxidation is not sufficiently reported in the literature (Tihay et al., 2011), while the analog studies on biomass-derived char oxidation could be approached (Amutio et al., 2012a; Fang et al., 2006; Li & Brown, 2001; Liang & Kozinski, 2000; Liu, 2002; Shen et al., 2009; Vaĭrhegyi et al., 2012; Yoon et al., 2012). The surface chemi-sorption of oxygen on carbon matrix was involved in the char oxidation kinetic model, concerning the evolution kinetics of CO and CO_2 (Li & Brown, 2001). The formation rate of CO_2 is more competitive than that of CO through the carbon-oxygen matrix ($^*C(O_2)$), giving the activation energy as 122 ± 12 kJ/mol for the reaction of powder charcoal sample. Most kinetic models for char oxidation incorporated the partial pressure of oxygen in reaction rate equation (Eq. (3)) (Liang & Kozinski, 2000; Tihay et al., 2011; Vaĭrhegyi et al., 2012), instead of the involvement of chemi-sorption kinetic process (such as L-H kinetic model (Gómez-Barea et al., 2005; Ollero et al., 2002)). The exponential factor for char in Eq. (3) (*nchar*) was all around 1 for three kinds of biomass-derived char oxidation reported by Vaĭrhegyi et al. (2012), confirming the assumption of this work ($n_{char} = 1$). The activation energy for the oxidation of three char samples was reported from 120 kJ/mol to 169 kJ/mol, which is higher than those obtained in this work (from 88.7 kJ/mol for 7% O_2 to115.1 kJ/mol for 60% O_2). The notable difference was on exponential factor for oxygen partial pressure (n_{oxy} from 0.5 to 0.73), which is much lower than that in this work ($n_{oxy} = 2.26$). Tihay et al. reported that the n_{char} of 2.07, activation energy of 173.9 kJ/mol and n_{oxy} of 1.16 was obtained for the best-fit case of cellulose-derived char oxidation during cellulose wadding process. The differences on the kinetic parameters for char oxidation among reported studies are mainly attributed to the origins, operating conditions and calculation methods.

The activation energy for cellulose-derived char oxidation during 455–522 °C was reported as 133.3 kJ/mol, without considering the effect of partial pressure of oxygen in kinetic model (Yoon et al., 2012). A number of separate-stage kinetic models for cellulose-derived char oxidation produced similar activation energies as those obtained in this work (Amutio et al., 2012a; Bilbao et al., 1997; Branca & Blasi, 2004). It needs to be clarified that the discrimination of two separate stages for cellulose degradation under oxidative atmosphere was not correlated with the bottom point of DTG curves (Tables 1 and 3). The selection of temperature range corresponding to the stages for calculation of kinetic parameters is dependent of the best linearity of the regression. This arbitrary discrimination may lead to the ambiguity of intrinsic reaction mechanism of the mass loss plateau (between about 380 °C and 440 °C), and limit the utilization of the separate-stage kinetic model for the process.

4. Conclusions

The cellulose degradation under inert and oxidative atmospheres was intensively discussed by means of TG-MS analysis, concerning the mass loss history and evolution of prominent volatiles and light gases. One more mass loss stage in high temperature stage was observed with addition of oxygen due to char oxidation, while effect of oxygen on low temperature stage was to promote the gas-phase reactions for production of light gases. The activation energy for char oxidation was increased with the oxygen concentration, while that for cellulose pyrolysis stage was slightly changed from analysis of the two-stage reaction kinetic model.

Acknowledgements

The authors greatly acknowledge the funding support from the projects supported by National Basic Research Program of China (973 Program) (Grant Nos. 2012CB215306 and 2010CB732206), National Natural Science Foundation of China (Grant No. 51106030) and Jiangsu University Natural Science Basic Research Program projects (12KJB480005).

References

Amutio, M., Lopez, G., Aguado, R., Artetxe, M., Bilbao, J., & Olazar, M. (2012). Kinetic study of lignoncellulosic biomass oxidative pyrolysis. *Fuel*, *95*, 305–311.
Amutio, M., Lopez, G., Aguado, R., Bilbao, J., & Olazar, M. (2012). Biomass oxidative flash pyrolysis: Autothermal operation, yields and product properties. *Energy and Fuels*, *26*, 1333–1362.
Antal, M. J., & Varhegyi, G. (1995). Cellulose pyrolysis kinetics: the current state of knowledge. *Industrial and Engineering Chemistry Research*, *34*, 703–717.
Bilbao, R., Mastral, J. F., Aldea, M. E., & Ceamanos, J. (1997). Kinetic study for the thermal decomposition of cellulose and pine sawdust in an air atmosphere. *Journal of Analytical and Applied Pyrolysis*, *39*, 53–64.
Blasi, C. D. (2008). Modeling chemical and physical processes of wood and biomass pyrolysis. *Progress in Energy and Combustion Sciences*, *34*, 47–90.
Branca, C., & Blasi, C. D. (2004). Global interinsic kinetics of wood oxidation. *Fuel*, *83*(1), 81–87.
Chandrasekaran, S. R., & Hopke, P. K. (2012). Kinetics of switch grass pellet thermal decomposition under inert and oxidizing atmospheres. *Bioresource Technology*, *125*, 52–58.
Dumitriu, S. (2005). *Polysaccharides: Structures diversity and functional versatility* (2nd ed.). New York: Marcel Dekker.
Fang, M. X., Shen, D. K., Li, Y. X., Yu, C. J., Luo, Z. Y., & Cen, K. F. (2006). Kinetic study on pyrolysis and combustion of wood under different oxygen concentrations by using TG-FTIR analysis. *Journal of Analytical and Applied Pyrolysis*, *77*, 22–27.
Gómez-Barea, A., Ollero, P., & Arjona, R. (2005). Reaction-diffusion model of TGA gasification experiments for estimating diffusional effects. *Fuel*, *84*, 1695–1704.
Huang, Y. F., Kuan, W. H., Chieuh, P. T., & Lo, S. L. (2011). Pyrolysis of biomass by thermal analysis–mass spectrometry (TA–MS). *Bioresource Technology*, *102*, 3527–3534.
Kashiwagi, T., & Nambu, H. (1992). Global kinetic constants for thermal oxidative degradation of a cellulosic paper. *Combustion and Fame*, *88*, 345–368.

Li, C., & Brown, T. C. (2001). Carbon oxidation kinetics from evolved carbon oxide analysis during temperature-programmed oxidation. *Carbon*, *39*, 725–732.
Liang, X. H., & Kozinski, J. A. (2000). Numerical modeling of combustion and pyrolysis of cellulosic biomass in thermogravimetric systems. *Fuel*, *79*, 1477–1486.
Lin, Y. C., Cho, J., Tompsett, G. A., Westmoreland, P. R., & Huber, G. W. (2009). Kinetics and mechanism of cellulose pyrolysis. *Journal of Physical Chemistry C*, *113*, 20097–20107.
Liu, N. A. (2002). Kinetic modeling of thermal decomposition of natural cellulosic materials in air atmosphere. *Journal of Analytical and Applied Pyrolysis*, *63*, 303–325.
Lv, G. J., & Wu, S. B. (2012). Analytical pyrolysis studies of corn stalk and its three main components by TG-MS and Py-GC/MS. *Journal of Analytical and Applied Pyrolysis*, *97*, 11–18.
McKendry, P. (2002a). Energy production from biomass (part 1): Overview of biomass. *Bioresource Technology*, *83*, 37–46.
McKendry, P. (2002b). Energy production from biomass (part 2): Conversion technologies. *Bioresource Technology*, *83*, 47–54.
Mettler, M. S., Vlachos, D. G., & Dauenhauer, P. J. (2012). Top ten fundamental challenges of biomass pyrolysis for biofuels. *Energy and Environmental Science*, *5*, 7797–7809.
Moulijn, J. A., & Kapteijn, F. (1995). Towards a unified theory of reactions of carbon with oxygen-containing molecules. *Carbon*, *33*, 1155–1165.
Ollero, P., Serrera, A., Arjona, R., & Alcantarilla, S. (2002). Diffusional effects in TGA gasification experiments for kinetic determination. *Fuel*, *81*, 1989–2000.
Ollero, P., Serrera, A., Arjona, R., & Alcantarilla, S. (2003). The CO_2 gasification kinetics of olive residue. *Biomass and Bioenergy*, *24*, 151–161.
Sanchez-Silva, L., Lopez-Gonzalez, D., Villasenor, J., Sanchez, P., & Valverde, J. L. (2012). Thermogravimetric-mass spectrometric analysis of lignocellulosic and marine biomass pyrolysis. *Bioresource Technology*, *109*, 163–172.
Sanderson, K. (2006). US biofuels: A field in ferment. *Nature*, *444*, 673–676.
Shen, D. K., & Gu, S. (2009). The mechanism for thermal decompostion of cellulose and its main products. *Bioresource Technology*, *100*, 6496–6504.
Shen, D. K., Gu, S., Luo, K. H., Bridgwater, A. V., & Fang, M. X. (2009). Kinetic study on thermal decomposition of woods in oxidative environment. *Fuel*, *88*, 1024–1030.
Shen, D. K., Hu, J., Xiao, R., Zhang, H. Y., Li, S. F., & Sai, G. (2012). Online evolved gas analysis by thermogravimetric-mass spectroscopy for thermal decomposition of biomass and its components under different atmospheres: Part I. Lignin. *Bioresource Technology*, http://dx.doi.org/10.1016/j.biortech.2012.11.081
Tihay, V., Boulnois, C., & Gillard, P. (2011). Influence of oxygen concentration on the kinetics of cellulose wadding degradation. *Thermochimica Acta*, *525*, 16–24.
Vaĭrhegyi, G., Sebestyeĭn, Z., Czegeĭny, Z., Lezsovits, F., & Könczöl, S. (2012). Combustion kinetics of biomass materials in the kinetic regime. *Energy and Fuels*, *26*, 1323–1335.
Widyawati, M., Church, T. L., Florin, N. H., & Harris, A. T. (2011). Hydrogen synthesis from biomass pyrolysis with in situ carbon dioxide capture using calcium oxide. *International Journal of Hydrogen Energy*, *36*, 4800–4813.
Yoon, H. C., Pozivil, P., & Steinfeld, A. (2012). Thermogravimetric pyrolysis and gasification of lignocellulosic biomass and kinetic summative law for parallel reactions with cellulose, xylan, and lignin. *Energy and Fuels*, *26*, 357–364.